Rupture of the Hydrogen Bond Linking Two Ω-Loops Induces the Molten Globule State at Neutral pH in Cytochrome *c*†

Federica Sinibaldi,‡ M. Cristina Piro,‡ Barry D. Howes,§ Giulietta Smulevich,§ Franca Ascoli,‡ and Roberto Santucci*,‡

Dipartimento di Medicina Sperimentale e Scienze Biochimiche, Università di Roma "Tor Vergata", via Montpellier 1, 00133 Roma, Italy, and Dipartimento di Chimica, Università degli Studi di Firenze, via della Lastruccia 3, 50019 Sesto Fiorentino, Italy

Received January 23, 2003; Revised Manuscript Received April 8, 2003

ABSTRACT: His26Tyr and His33Tyr mutants were obtained from the Cys102Thr variant of yeast iso-1-cytochrome *c*. Spectroscopic studies show that a mutation at position 26 at pH 7.0 enhances flexibility of the peptide, alters the heme pocket region and the axial coordination to heme-iron, and reduces protein stability. The His26Tyr mutant shows properties typical of the molten globule. Further, formation of an axially misligated minor low spin species occurs with partial displacement of Met80, the axial ligand of the heme-iron in the native protein. The pK_a determined for the alkaline transition of this mutant is 7.48 (± 0.05), approximately 0.5 lower than that of the wild-type protein. Hence, the alkaline conformer is populated at pH 7.0, and the sixth ligand of the misligated species is proposed to be a lysine. Furthermore, a reduction in catalytic activity indicates that the functional properties are altered. The results suggest that the structural and functional changes observed in the His26Tyr mutant are because the mutation frees the two Ω-loops that, in the native protein, are linked by the hydrogen bond between His26 and Glu44. Hence, one may infer that the His26−Glu44 hydrogen bond is essential for the rigidity and stability of the native protein. In its absence, the heightened flexibility of the peptide fold results in conversion of the macromolecule to a molten globule state, even at neutral pH. Ligand exchange at the sixth coordination position of the heme-iron(III) observed as the minor species (i.e., the alkaline conformer) is therefore induced by a long-range effect. This result is of interest since mutations reported to date, which stabilize the alkaline conformer, all occur in the loop including Met80. By contrast, only very minor spectroscopic (and, thus, structural) changes are observed for the His33Tyr mutant. This suggests that His33 does not form intramolecular bonds considered important for the protein structure and stability, and is consistent with the high variability of residues at position 33 in cytochromes *c*.

Cytochrome *c* (cyt *c*),[1] perhaps the most studied example of the class of heme proteins, is a single polypeptide containing the heme prosthetic group covalently bound to Cys14 and Cys17 via two thioether linkages. Studies on mutants of cyt *c* have provided important information concerning the role played by side chains (in particular, the invariant residues) in terms of structural stabilization, folding, and regulation of the functional properties (*1*−*7*). In this context, yeast iso-1-cyt *c* represents an ideal model-system for cytochromes *c*; a high-resolution X-ray structure of the protein is available (*8*), and a system to generate mutants by direct mutagenesis has been developed (*9*, *10*).

In the present paper, we exploit the potential offered by site-directed mutagenesis to alter specific interactions in the protein and, consequently, gain insight into the role of such interactions. In particular, we investigate the properties of iso-1-cyt *c* modified at positions 26 or 33. The histidines that occupy these positions in the wild-type (wt) form are replaced by a tyrosine giving the His26Tyr and His33Tyr mutants. The interest in His26, which is located in the 20s omega (Ω)-loop (residues 18−31), lies in the fact that it is an invariant residue in vertebrate and higher plant cytochromes *c*. Moreover, in the native protein, the imidazole group of His26 is hydrogen bonded to Asn31 (forming an intraloop interaction) and to the backbone carbonyl of Glu44 (Pro44 in horse cyt *c*), thus forming a bridge between the 20s and the 40s Ω-loops of the polypeptide chain (Figure 1).

The His26−Glu44 (Pro44 in horse cyt *c*) hydrogen bond present in the native protein is missing in the acidic molten globule state (called the A-state), due to protonation of the histidine side chain at the pH investigated (pH 2.2). With respect to the native protein, the molten globule possesses native-like α-helix secondary structure but fluctuating tertiary conformation (*11*−*13*); therefore, it shows enhanced flexibility that, in the case of the A-state, is ascribed mostly to the loop regions of the polypeptide (*5*, *14*, *15*).

† Research funded in part by grants from Italian MIUR (COFIN 2001 031798).

* To whom correspondence should be addressed: Dipartimento di Medicina Sperimentale e Scienze Biochimiche, Università di Roma "Tor Vergata", Via Montpellier 1, 00133 Roma (Italy). Fax: + 39 06 72596353. E-mail: santucci@med.uniroma2.it.

‡ Università di Roma "Tor Vergata".

§ Università degli Studi di Firenze.

[1] Abbreviations: cyt *c*, cytochrome *c*; LS, low-spin; HS, high-spin; circular dichroism, CD; resonance Raman, RR; wild-type, wt.

10.1021/bi034132r CCC: $25.00
Published on Web 05/24/2003

FIGURE 1: Ribbon structure of yeast iso-1-cyt *c* (Cys102Thr). The hydrogen bond of His26 to the carbonyl group of Glu44 (Pro in horse cyt *c*) is shown. The structure (*44*) was visualized with the Swiss-Pdb Viewer software (*45*).

The present work compares the structural and functional properties of the His26Tyr and His33Tyr mutants of cyt *c* under physiological-like conditions, and has a dual objective: (i) to establish the role played by the His26−Glu44 (Pro44 in horse cyt *c*) hydrogen bond in the stabilization of the rigid tertiary conformation of the native protein, and (ii) to determine if the lack of this hydrogen bond induces the protein to assume a molten globule-like structure at neutral pH. On the other hand, since position 33 in cytochromes *c* is not highly conserved and the His33 residue does not form any intramolecular bonds considered important for the protein structure and stability, no marked effects are expected upon mutation.

MATERIALS AND METHODS

Protein Expression and Purification. The expression plasmid pBTRI harboring both the yeast iso-1-cyt *c* gene (*CYC1*) and heme lyase gene (*CYC3*) was a kind gift from A. Grant Mauk of the British Columbia University at Vancouver. The *CYC1* gene encodes the Cys102Thr variant of yeast iso-1-cyt *c*. In this variant, protein dimerization is precluded and the ferricytochrome autoreduction rate is greatly diminished; on the other hand, the optical and electrochemical properties are indistinguishable from those of the wt protein (*9*).

Site-directed mutagenesis of the *iso*-1-cyt *c* gene (Cys102Thr variant) was performed directly on the pBTRI plasmid. Specific amino acid substitutions (His26Tyr and His33Tyr) were introduced in yeast *iso*-1-cyt *c* using the GeneEditor kit "In Vitro Site Directed Mutagenesis System" (Promega, Madison WI) and the following oligonucleotides (M-Medical, Italy), where letters in bold indicate base changes in codons 26 or 33 of the iso-1-cyt *c* gene.

His26Tyr mutant 5′-GGT GGC CCA **T**AT AAG GTT G-3′

His33Tyr mutant 5′-CCA AAC TTG **T**AT GGT ATC-3′

Bacterial expression and purification of the recombinant proteins were conducted essentially as described in ref *10* with minor modifications.

Escherichia coli strain JM 109 containing the pBTRI plasmid (or the mutated plasmids, see above) was grown at 37 °C, in 2 L of SB medium containing 100 μg/mL ampicillin to an absorbance of 0.3 OD at 600 nm. Induction was accomplished by adding IPTG (isopropyl-β-D-thiogalactopyranoside) to a final concentration of 0.75 mM. Cells were incubated at 37 °C overnight, harvested by centrifugation, and frozen at −80 °C. After thawing, the reddish pellets were resuspended in 50 mM Tris pH 8 (3−4 mL/g of wet cells). Lysozyme (1 mg/mL) and DNase (5 μg/mL) were added to the homogenized cells. The suspension was left in ice for 1 h and then sonicated for 1 min, at medium intensity, 50% duty cycle. After centrifugation of the sample for 30 min at 10000*g* to remove cell debris, the clarified supernatant was dialyzed overnight against 10 mM phosphate buffer pH 6.2 and then loaded on a CM 52 column (40 mL bed volume) equilibrated with the same buffer. Purification was performed by washing the column with one volume of 45 mM phosphate pH 6.8, then one volume of 45 mM phosphate pH 6.8, 75 mM NaCl and by eluting the protein with one volume of 45 mM phosphate pH 6.8, 250 mM NaCl. After purification, the recombinant C102T variant of yeast iso-1-cyt *c* (indicated herein as "wt" protein) and the His26Tyr and the His33Tyr mutated proteins (yield 5−7.5 mg/L) were promptly oxidized by adding a few grains of potassium ferricyanide and then subjected to extensive dialysis against 100 mM phosphate buffer pH 7.0. The recombinant proteins (∼500 μM) were more than 98% pure (from SDS−PAGE analysis and reverse phase HPLC, data not shown) and stored at −80 °C in 200 μL aliquots.

Circular Dichroism (CD) Measurements. Measurements were carried out at 25 °C using a Jasco J-710 spectropolarimeter (Tokyo, Japan) equipped with a PC as data processor. The molar ellipticity [θ] (deg cm^2 dmol^{-1}) is expressed on a molar heme basis in the Soret (380−450 nm) and near-UV (270−300 nm) regions, and as mean residue ellipticity in the far-UV region (200−250 nm, mean residue molecular mass = 119).

Electronic Absorption Measurements. Electronic absorption measurements were carried out at 25 °C using a Cary 5 spectrophotometer. Cyt *c* concentration was determined on the basis of the extinction coefficient $\epsilon = 106$ mM^{-1} cm^{-1} at 408 nm.

Resonance Raman Measurements. Resonance Raman (RR) spectra were obtained at room temperature with excitation from the 406.7 nm line of a Kr^+ laser (Coherent, Innova 90/K). The backscattered light from a slowly rotating NMR tube was collected and focused into a computer-controlled double monochromator (Jobin-Yvon HG2S) equipped with a cooled photomultiplier (RCA C31034A) and photon counting electronics. To minimize local heating of the protein by the laser beam, the sample was cooled by a gentle flow of N_2 gas passed through liquid N_2. RR spectra were calibrated to an accuracy of 1 cm^{-1} for intense isolated bands with indene as the standard for the high-frequency region and with indene and CCl_4 for the low-frequency region.

Cyclic Voltammetry Measurements. Voltammetric measurements were performed at 25 °C in a glass microcell (sample volume: 1 mL) equipped with a reference calomel electrode ($E = 244$ mV vs NHE, at 25 °C; Amel, Milan, Italy), a Pt wire as the counter-electrode and a gold electrode (2 mm diameter, Amel) with adsorbed 4,4′-bipyridine (Merck, Germany) (*16*), as the working electrode.

An Amel 433/W multipolarograph (Milan, Italy) interfaced with a PC was employed for voltammetric measurements. Before the voltammetric experiment, the solution was

deaerated for 30 min by a gentle flow of pure nitrogen maintained just above the solution surface.

Catalytic Activity Measurements. Polarographic measurements were carried out at room temperature using a Clark-type O_2 electrode (Ysi mod. 5300, Yellow Springs, OH) interfaced with a recorder. The oxygen probe was inserted into a 0.6 mL chamber (Instech Laboratories, mod. 600A, Horsham, PA) containing 57 nM bovine cytochrome *c* oxidase dissolved in 50 mM phosphate buffer, pH 7.0, in the presence of 10 mM ascorbate and 0.23 mM *N*,*N*,*N*′,*N*′-tetramethyl-*p*-phenylenediamine (TMPD). Increasing amounts of the protein were then added, and slope changes recorded. Catalytic activities were calculated as turnover numbers, from the rates corrected for the nonenzymatic oxygen consumption.

Guanidine Hydrochloride(Gdn-HCl)-Induced Denaturation. Protein unfolding was carried out by incrementally increasing the Gdn-HCl concentration in a single sample of the protein (concentration: 7 μM), taking into account the dilution factors. The protein was equilibrated in denaturant at room temperature for a minimum of 20 min before each measurement.

pH Measurements. A Crison 2001 pHmeter (Alella, Spain) was used for pH measurements.

RESULTS

His26 is located in the Ω-loop adjacent to the heme pocket region, indicated as the 20s loop (see Figure 1). In a manner similar to the protein purified from horse heart, in iso-1-cyt *c* the hydrogen bond of His26 with the carbonyl group of Glu44 (Pro44 in horse cyt *c*) contributes to the rigidity and stability of the protein structure, joining the 20s and 40s loop regions (*8*). Substitution of the histidine with another amino acid may alter the 20s loop conformation and weaken (or induce the rupture of) the hydrogen bond between residues 26 and 44, thus freeing the two Ω-loops and increasing the macromolecule flexibility (*17*−*19*). In the present work, the His26Tyr mutant has been characterized, and the effect of this mutation on the polypeptide tertiary structure was investigated. The data are compared with those obtained for the His33Tys mutant, a residue that does not form any intramolecular bonds considered important for the protein structure and stability.

Circular Dichroism. His26Tyr and His33Tyr mutants of iso-1-cyt *c* show well-defined far-UV dichroic spectra (not shown), typical of proteins with α-helix secondary structure, of ellipticity comparable to that of the wt form. The Soret CD spectra (400−450 nm, related to the structure of the heme pocket) are shown in Figure 2. The His33Tyr spectrum is practically indistinguishable from the wt, whereas that of the His26Tyr mutant shows a weakened 416 nm Cotton effect. This signal, attributed to the Phe82− and Met80−heme interaction (*20*, *21*), is considered diagnostic for the environment near the Met80−Fe(III) axial bond in the native protein. Therefore, the decreased 416 nm Cotton effect in the His26Tyr mutant may reveal (i) an increased distance between the residues Phe82, Met80, and the heme group, as consequence of an enhanced mobility of the 70−85 residues segment, or (ii) the presence of a minor species with X−Fe−His18 axial coordination (where X is a misligated endogeneous ligand) in equilibrium with the protein having Met80

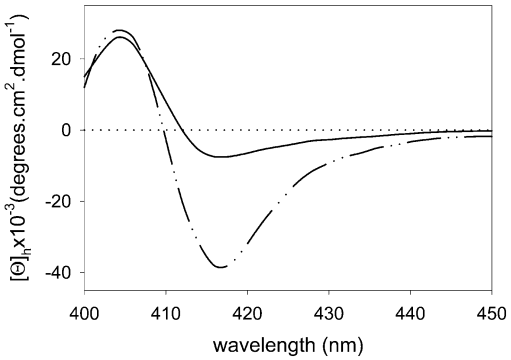

FIGURE 2: Soret CD spectra of the His26Tyr (—) and His33Tyr (—••—) mutants of yeast iso-1-cyt *c*; the latter is identical to the spectrum of the wild type form (not shown). Experimental conditions: 0.1 M phosphate buffer, pH 7.0 at 25 °C.

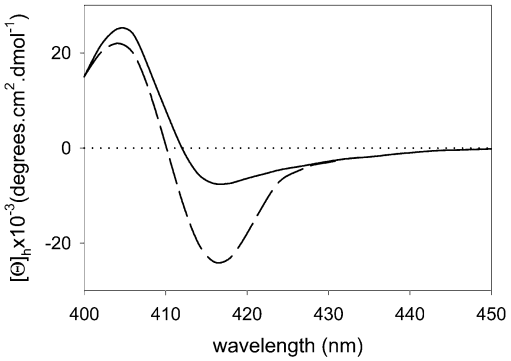

FIGURE 3: Soret CD spectrum of the His26Tyr mutant at 25 °C (—) and 5 °C (— — —). The temperature-dependent transition proved to be fully reversible. Other experimental conditions are as described in Figure 2.

as sixth coordination ligand. In the latter case, only the fraction of macromolecules with Met80−Fe−His coordination will contribute to the 416-nm dichroic signal. The near-UV CD spectrum of the His26Tyr mutant (not shown) shows a slightly weaker signal, indicating a decreased interaction between Trp59 and a heme-propionate, and consistent with an increased distance between the two groups.

The Soret CD spectrum of the His26Tyr mutant at 25 °C is similar to that of the A-state of cyt *c* (*22*). This suggests that, like the A-state, the mutant possesses enhanced flexibility with respect to the wt protein. Therefore, CD of the His26Tyr mutant was performed at 5 °C, at which reduced macromolecule flexibility is expected. The far-UV CD spectrum of the mutant remains unaffected (therefore indicating an unchanged secondary structure); conversely, the negative 416-nm Cotton effect (Figure 3) shows a significant increase in ellipticity at 5 °C. Furthermore, the temperature-induced transition is fully reversible. This result indicates that the tertiary structure of the His26Tyr mutant is fluctuating at room temperature as consequence of the increased flexibility of the two loops linked in the native state by the His26−Glu44 hydrogen bond (see Figure 1). Moreover, the temperature-dependence of the 416-nm ellipticity suggests that, at room temperature, the enhanced protein flexibility leads to increased mobility of the loop containing Met80, therefore hindering methionine coordination to the heme-iron.

Electronic Absorption and Resonance Raman. A comparison of the electronic absorption and resonance Raman

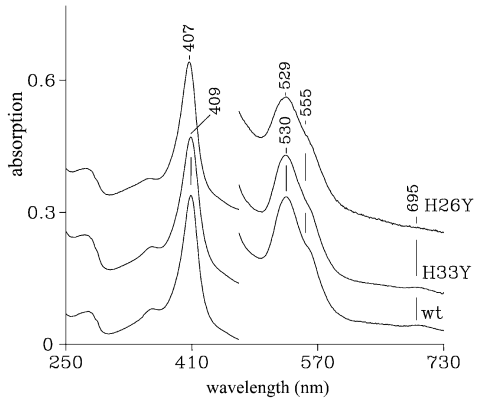

FIGURE 4: Electronic absorption spectra of wt iso-1-cyt *c* and the His26Tyr and His33Tyr mutants. Experimental conditions: sample concentration, 35 μM; 0.1 M phosphate buffer, pH 7.0 at 25 °C. The visible region is expanded 8-fold. The path length of the cuvette was 1 mm for all spectra. The ordinate scale refers to the wt protein.

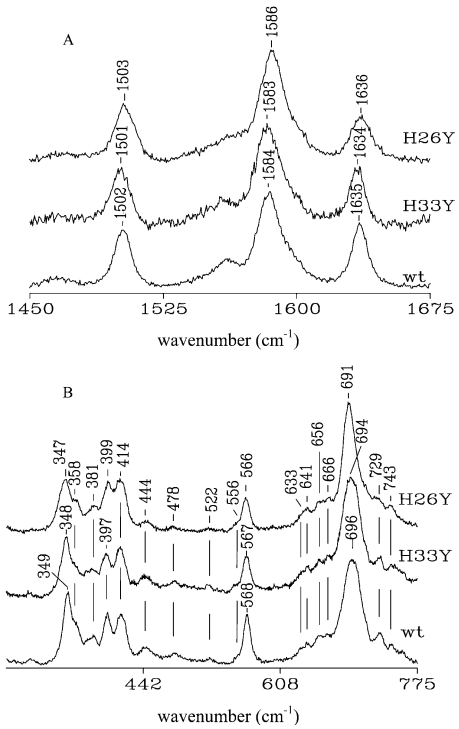

FIGURE 5: Resonance Raman spectra of wt iso-1-cyt *c* and the His26Tyr and His33Tyr mutants in 0.1 M phosphate, pH 7.0. Experimental conditions: sample concentration, 35 μM; 5 cm^{-1} resolution; 406.7 nm excitation; 15 mW laser power at the sample; (A) high-frequency region: (wt) 21 s/0.5 cm^{-1} collection interval; (His33Tyr) 12 s/0.5 cm^{-1} collection interval; (His26Tyr) 16 s/0.5 cm^{-1} collection interval; (B) low-frequency region: (wt) 14 s/0.5 cm^{-1} collection interval; (His33Tyr) 6 s/0.5 cm^{-1} collection interval; (His26Tyr) 8 s/0.5 cm^{-1} collection interval.

spectra of the His26Tyr and His33Tyr mutants with the wt protein is shown in Figures 4 and 5, respectively. It is immediately apparent that the absorption spectrum of His33Tyr is essentially identical to that of the wt, whereas the spectrum of His26Tyr is slightly blue-shifted. Furthermore, the band at 695 nm, which is considered as a diagnostic indicator of the integrity of the Met80−Fe(III) bond (*23*), is clearly discernible in His33Tyr but very weak in His26Tyr. The RR spectrum of the wt protein is very similar to that observed for native horse heart cytochrome *c* at pH 7.0, characterized by a low spin (LS) heme spin state (*24*−*26*). The RR frequencies of the core size marker bands of His33Tyr (Figure 5A) are downshifted by 1 cm^{-1}, while those of the His26Tyr mutant are slightly upshifted compared to the wt protein. There is no evidence for high spin (HS) species. This indicates, in accord with the CD and absorption spectra, that the heme properties of His33Tyr are very similar to wt. The upshift of the RR frequencies for His26Tyr and the slight asymmetry of the ν_3 band (1503 cm^{-1}) suggests the presence of a minor LS species with Lys−His (*27*) or bis-His (*25*, *28*) axial iron coordination, a possibility that is in accord with CD data (Figure 2). The change of axial coordination from Met−His to bis-His for cytochromes *c*, leading to a blue shift of the absorption spectrum and an upshift of the RR marker band frequencies, has been associated with a more relaxed heme distortion (*25*, *28*). A similar effect may also be responsible for the changes observed in the case of Lys−His coordination. Studies of heme model compounds have also shown that an increase in the degree of heme distortion gives rise to a red shift of the absorption spectrum (*29*). Further support for a more relaxed heme distortion in His26Tyr compared to the wt protein can be found in the low-frequency RR spectrum (Figure 5B). This region of the RR spectrum is characterized by vibrations of the heme peripheral substituents and porphyrin out-of-plane modes. The spectra of Figure 5B are very complex as the substituent and out-of-plane RR modes become active in cyt *c* as a consequence of the distorted heme. The distortion being imposed by interaction with the protein matrix through covalent thioether links between the heme and two cysteine residues (*30*, *31*). The intensity and frequency of a number of bands in His26Tyr are significantly different compared to the wt. In particular, changes are evident for bands at 444, 568, and 729 cm^{-1}. By analogy with horse heart cyt *c*, these bands are assigned to the out-of-plane modes γ_{22}, γ_{21}, and γ_5, respectively (*31*). Furthermore, variations are clear for vibrations associated with the thioether linkages at 397 cm^{-1} [δ(C$_\beta$C$_a$S)] and 696 cm^{-1} [ν(C−S)]. Similar changes have been reported previously for cytochromes *c* upon change of axial coordination which reduce the heme distortion (*24*, *25*, *28*, *32*). In horse heart cyt *c*, the band centered at 696 cm^{-1} is reported to be composed of two modes, ν(C−S) and ν_7. The latter mode, at 701 cm^{-1} in the native protein, is observed to downshift when the heme distortion relaxes, overlapping better with the ν(C−S) mode resulting in a sharpening of the band (*32*). A similar effect may be active in the case of the His26Tyr mutant, contributing to the observed downshift and narrowing of the band at 696 cm^{-1} in the spectrum of the wt. Less dramatic changes are evident in the spectrum of His33Tyr compared to wt, indicating that the reduction in heme distortion is less pronounced. The similarity of the high-frequency RR spectrum to that of wt suggests that these small variations are not due to a change of axial coordination. Hence, the more relaxed heme distortion in this case may result from a change in conformation of the peptide loops near the porphyrin macrocycle which perturb the thioether bonds with the heme.

To shed further light on the identity of the axial ligand in the misligated species of His26Tyr, a spectrophotometric titration of the 695 nm absorbance band as a function of pH (range: 6.0−10.5, data not shown) was carried out to establish whether the His26Tyr mutation affects the pK_a of

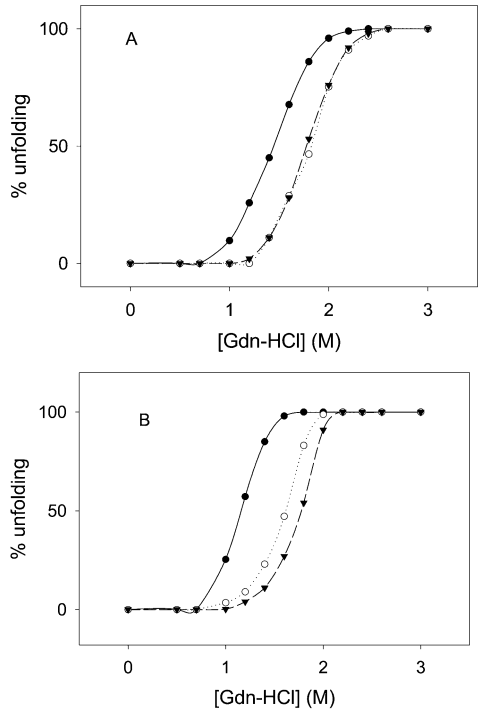

FIGURE 6: Unfolding profiles of the His26Tyr (●) and His33Tyr (○) mutants of yeast iso-1-cyt *c*. Experimental points are obtained from dichroic measurements carried out at 222 nm (panel A) and 408 nm (panel B), as a function of Gdn-HCl concentration. The unfolding profiles of the wild type form (▼) are also shown for comparison. Other experimental conditions are as described in Figure 2.

the protein alkaline transition. A pK_a = 7.48 (± 0.05) was determined, which is approximately 0.5 lower than observed for the wt protein (*10*). Hence, it is apparent that the mutation stabilizes the alkaline conformer such that it is populated at pH 7.0 and, consequently, coordination of a Lys rather than His residue is favored.

Stability of the His26Tyr and His33Tyr Mutants. The thermodynamic stability of the His26Tyr and His33Tyr mutants was investigated by following protein unfolding induced by Gdn-HCl. The denaturation profiles of the His26Tyr and His33Tyr mutants (as monitored by CD) in the presence of Gdn-HCl, are shown in Figure 6. Changes in ellipticities are expressed as percentage of unfolding. The experimental points refer to ellipticity measured at 222 nm (a probe for the α-helix structure, panel A) and 408 nm (a probe for the structure at the heme pocket, panel B). The thermodynamic parameters of the transitions are reported in Table 1. Some values of the wt differ from those previously reported (*33*); this may be explained by considering that the spectroscopic techniques employed (CD herein, fluorescence in ref *33*) monitor different regions of the macromolecule. In the far-UV region, the unfolding profile of the His33Tyr mutant overlaps that of the wt form, whereas that of the His26Tyr mutant appears shifted toward lower denaturant concentration, therefore indicating a decreased stability. This is confirmed by the values of the apparent free energy change (ΔG_D) obtained from the apparent denaturation equilibrium constant, K_D (determined by the expression $K_D = (\theta_i - \theta_{obs})/(\theta_{obs} - \theta_f)$, where θ_i, θ_f, and θ_{obs} represent the initial, final, and observed values of ellipticity, respectively). Values of ΔG_o, i.e., the apparent free energy change in the absence of denaturant, were estimated by extrapolating the curves to zero denaturant concentration, on the assumption of a linear dependence of the ΔG_D versus denaturant concentration (*34*). The ΔG_o value of the His26Tyr mutant is significantly lower than that of the His33Tyr mutant and of the wild-type protein. A similar trend is observed from analysis of the Soret data, where the His26Tyr mutant again shows decreased stability with respect to the wild type protein. In this region, the His33Tyr mutant also shows a slightly decreased stability, indicating that mutation at position 33 may have some effect on the heme pocket region of the protein. The values of *m*, a parameter that directly measures the dependence of ΔG_D on the denaturant concentration ([D]) according to the empirical equation $\Delta G_D = \Delta G_o - m[D]$ are in good agreement with the data obtained. The His26Tyr mutant, in fact, shows a value of *m* (that is assumed to be proportional to the change of accessible area of a protein upon unfolding (*34*, *35*) lower than that of the His33Tyr mutant and the wt form. This is consistent with a decreased structural compactness of the His26Tyr mutant.

Table 1: Denaturation Parameters[a] of the His26Tyr and His33Tyr Mutants of iso-1-cyt *c*[b]

	$C_{1/2}$[c] (M)	ΔG_o (kJ/mol)	m (kJ/mol/M)
	wt		
helix region	1.8	22.4	12.4
Soret region	1.8	22.2	12.3
	His33Tyr mutant		
helix region	1.8	22.4	12.4
Soret region	1.6	19.7	12.0
	His26Tyr mutant		
helix region	1.4	14.8	10.1
Soret region	1.1	13.4	10.0

[a] Experimental conditions: 0.1 M phosphate buffer, pH 7.0, and 25 °C. [b] Thermodynamic parameters of various transitions are determined from CD studies. The estimated errors in $C_{1/2}$, ΔG_o, and *m* are ± 0.1 M, ± 1.1 kJ/mol, and ± 0.9 kJ/mol/M, respectively. [c] Denaturant concentration at the transition point.

Redox Properties. The redox properties of the His26Tyr mutant were determined by using dc cyclic voltammetry. Like horse cyt *c* (*16*, *36*), yeast iso-1- cyt *c* and the His26Tyr mutant exhibit a well-defined electrochemistry at a gold electrode chemically modified with 4−4′-bipyridine. In the 20−200 mV s^{-1} scan rate range, cyclic voltammograms of the His26Tyr mutant (one of which is shown in Figure 7) show cathodic and anodic peaks similar in shape and magnitude, anodic and cathodic peak current ratio (I_{pa}/I_{pc}) close to unity, and peak separation (ΔE_p) values (85−100 mV, depending on the scan rate) relatively close to the theoretical value (57 mV s^{-1}) expected for a fully reversible one-electron-transfer reaction at 25 °C (*37*). The calculated redox potential, $E_{1/2}$ = 274 (± 6) mV vs NHE, is very similar to that of the wt form ($E_{1/2}$ = 285 (± 6) mV vs NHE, in agreement with the value reported in ref *10*). This is in accord with the observation that the Met−Fe(III)−His axially coordinated form is the major component in solution.

To determine the behavior of the His26Tyr and His33Tyr mutants in the presence of biological reaction partners of the protein, we followed the redox reaction between the reduced mutants and cytochrome *c* oxidase. The reaction kinetics, performed as described in ref *36*, reveal that, whereas the His33Tyr activity is pratically identical to the

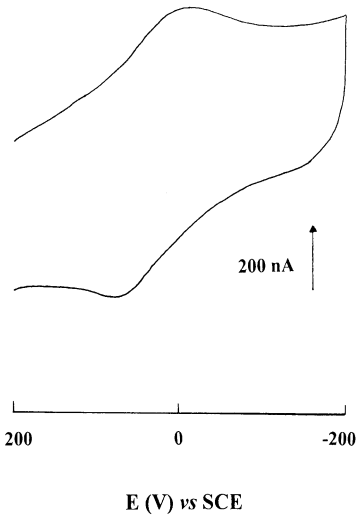

FIGURE 7: Dc cyclic voltammogram of the His26Tyr mutant of yeast iso-1-cyt *c* at a gold electrode chemically modified with 4,4′-bypiridine. Scan rate: 100 mV s^{-1}. Protein concentration: 0.1 mM. Other experimental conditions as in Figure 2.

wt form, that of the His26Tyr mutant is reduced (by approximately 20%), therefore indicating that mutation at position 26 reduces the capability of the protein to exchange electrons with biological partners.

DISCUSSION

Molten globules are compact states possessing native-like secondary structure but fluctuating tertiary conformation. These forms maintain some native tertiary contacts, but protein flexibility increases considerably. For cyt *c*, this may be ascribed mainly to the enhanced flexibility of Ω-loop regions, as a native-like hydrophobic core is found to be retained (*5*, *15*). Ω-loops are protein segments solely located at the protein surface and constituted mainly by polar amino acidic residues, devoid of a regular secondary structure and characterized by high flexibility and small distance between segment termini (*38*). In yeast iso-1-cyt *c*, the hydrogen bond between His26 and Glu44 (Pro44 in horse cyt *c*) links the 20s loop to the 40s loop; it is thus expected to contribute significantly to the stability and rigidity of the native state. The rupture of such hydrogen bond is thought to enhance fluctuations of the two loops that may also affect the Met80-containing segment and, consequently, weaken the Met80−Fe(III) axial bond.

The molten globule is considered a compact intermediate that forms during protein folding; therefore, the availability of a molten globule at neutral pH is of great importance. On the basis of data here reported, we propose that the His26Tyr mutation induces formation of a molten globule state of cyt *c* at neutral pH. Accordingly, compared to the wt protein, the His26Tyr mutant displays (i) an altered heme pocket region and axial coordination to heme-iron, (ii) enhanced peptide flexibility and reduced protein stability, and (iii) decreased biological activity. Further, the conformation of the His26Tyr mutant is modulated both by temperature (below 25 °C, Figure 3) and by anions (data not shown) at neutral pH, as previously observed for the A state (*22*). Therefore, it can be assumed that the disruption of the His26−Glu44 (Pro44 in horse cyt *c*) hydrogen bond induces the native protein to rearrange into a molten globule state.

The His26Tyr mutant is characterized by only LS states; therefore, it becomes an interesting system to study because of its entirely LS character. It provides the important advantage of enabling the equilibrium between the two LS configurations (X−Fe−His ⇆ Met−Fe−His, where X is the endogeneous ligand coordinated to the iron(III) in place of Met80) to be monitored without any interference from HS species (as is the case for the acidic molten globule (*39*)). This equilibrium, that is observed in the His26Tyr mutant but not in the His33Tyr mutant, can be envisaged as resulting from the enhanced flexibility of the macromolecule, which opposes Met80 coordination to the heme-Fe(III) and decreases the strength of the Met80 bond to the metal. This is confirmed by the observation that the X−Fe−His ⇆ Met−Fe−His equilibrium shifts toward the Met80−Fe−His form as the temperature is lowered.

The nature of the misligated axial ligand in the minor species observed in the His26Tyr mutant is of interest. Although our Raman data indicate a histidine or a lysine as the most likely candidates, the pK_a of its alkaline transition was found to be lowered by 0.5 compared to the wt protein expressed in *E. coli* (7.48 vs 7.95) (*10*). Hence, the misligated ligand of the heme-iron at pH 7.0 is proposed to be a lysine. It has previously been reported for the native protein that the alkaline conformer with Lys79 bound to the heme iron has very similar spectral characteristics to the neutral form, whereas the Lys73 bound alkaline conformer has more distinct features, including an upshift of the RR frequencies (*27*). Hence, Lys73 or Lys72, which is not trimethylated in the recombinant protein expressed in *E. coli* (*10*) and thus may bind to the heme iron, are considered to be the more likely lysine axial ligands.

The stabilization of the alkaline conformer at pH 7.0 is particularly interesting as the mutations reported to date that stabilize the alkaline conformer occur in the Ω-loop which includes Met80. Hence, further insight into the factors that determine formation of the alkaline conformer in cyt *c* may be forthcoming from consideration of the long-range effects that induce this state upon mutation of His26. The alkaline conformer is characterized by a globular fold with protein dimensions similar to the native state; however, it exhibits a more flexible structure, and the 20s and 40s loop regions appear among the regions that mostly differ from the native conformation. Recently, it has been proposed that the increased flexibility and consequent destabilization of the native fold is responsible for the change in axial ligand (*40*). The structural requisites necessary to effect the alkaline transition of native cyt *c* find close similarities in the increased mobility and structural destabilization of the native fold described herein for the His26Tyr mutant. In this regard, it is worthy of note that one characteristic of the molten globule state observed for this mutant is a misligated minor Lys/His conformer at pH 7.0. Hence, it is evident that the destabilization we have noted is not restricted to the heme environment alone, but has more extensive implications for the protein fold, including an enhanced mobility of the Met80-containing loop. The observation that chemical denaturants and high temperature decrease the pK_a of the alkaline transition, and thereby influence the protein unfolding mechanism (*41*, *42*), finds now reasonable explanation in the fact that these agents free the 20s and 40s loops through the rupture of the His26−Glu44 hydrogen bond.

Hence, our results support the view that an alkaline-like species may be involved in the cytochrome *c* folding pathway under native conditions (*40*−*42*).

By contrast, the properties of the His33Tyr mutant are in marked contrast with those of the His26Tyr mutant and are very similar to the wt, thus suggesting that mutation at position 33 does not induce changes of relevance in the conformation and the biological activity of the protein. This is consistent with the observation that His33 does not form intramolecular bonds considered important for the protein structure and stability and is in accord with the high variability of residues at position 33 in cytochromes *c* (*43*).

ACKNOWLEDGMENT

The authors wish to thank A. Grant Mauk (British Columbia University, at Vancouver) for supplying the yeast iso-1-cyt *c* expression plasmid, P. Sarti and E. Forte (Università di Roma "La Sapienza") for assistance in the polarographic measurements.

NOTE ADDED AFTER ASAP POSTING

This paper was inadvertently posted to the Web on 05/24/03 with the phrase "for both proteins)" included at the end of the first full sentence in the column of text under Table 1. The correct version of the paper was posted 05/30/03.

REFERENCES

1. Rafferty, S. P., Pearce, L. L., Barker, P. D., Guillemette, J. G., Kay, C. M., Smith, M., and Mauk, A. G. (1990) *Biochemistry 29*, 9365−9369.
2. Berghuis, A. M., Guillemette, J. G., Smith, M., and Brayer, G. D. (1994) *J. Mol. Biol. 235*, 1326−1341.
3. Lo, T. P., Guillemette, J. G., Louie, G. V., Smith, M., and Brayer, G. D. (1995) *Biochemistry 34*, 163−171.
4. Lo, T. P., Komar-Panicucci S., Sherman, F., McLendon G., and Brayer, G. D. (1995) *Biochemistry 34*, 5259−5268.
5. Marmorino, J. L., and Pielak, G. J. (1995) *Biochemistry 34*, 3140−3143.
6. Rafferty, S. P., Guillemette, J. G., Berghuis, A. M., Smith, M., Brayer, G. D., and Mauk, A. G. (1996) *Biochemistry 35*, 10784−10792.
7. Doyle, D. F., Waldner, J. C., Parikh, S., Alcazar-Roman, L., and Pielak, G. J. (1996) *Biochemistry 35*, 7403−7411.
8. Louie, G. V., and Brayer, G. D. (1990) *J. Mol. Biol. 214*, 527−555.
9. Cutler, R. L., Pielak, G. J., Mauk, A. G., and Smith, M. (1987) *Protein Eng. 1*, 95−99.
10. Pollock, W. B., Rosell, F. I., Twitchett, M. B., Dumont, M. E., and Mauk, A. G. (1998) *Biochemistry 37*, 6124−6131.
11. Goto, Y., Calciano, L. J., and Fink, A. L. (1990) *Proc. Natl. Acad. Sci. U.S.A. 87*, 573−577.
12. Goto, Y., Takahashi, N., and Fink, A. L. (1990) *Biochemistry 29*, 3480−3488.
13. Goto, Y., and Nishikiori, S. (1991) *J. Mol. Biol. 222*, 679−686.
14. Jeng, M. F., Englander, S. W., Elove, G. A., Wand, A. J., and Roder, H. (1990) *Biochemistry 29*, 10433−10437.
15. Marmorino, J. L., Lethi, M., and Pielak, G. J. (1998) *J. Mol. Biol. 275*, 379−388.
16. Frew, J. E., and Hill, H. A. O. (1988) *Eur. J. Biochem. 172*, 261−269.
17. Qin, W., Sanishvili, R., Plotkin, B., Schejter, A., and Margoliash, E. (1995) *Biochim. Biophys. Acta 1252*, 87−94.
18. Fetrow, J. S., Dreher, U., Wiland, D. J., Schaak, D. L., and Boose, T. L. (1998) *Protein Sci. 7*, 994−1005.
19. Rumbley, J. N., Hoang, L., and Englander, S. W. (2002) *Biochemistry 41*, 13894−13901.
20. Pielak, G. J., Oikawa, K., Mauk, A. G., Smith, M., and Kay, C. M. (1986) *J. Am. Chem. Soc. 108*, 2724−2727.
21. Ascoli, F., and Santucci, R. (1996) *J. Inorg. Biochem. 68*, 211−214.
22. Santucci, R., Bongiovanni, C., Mei, G., Ferri, T., Polizio, F., and Desideri, A. (2000) *Biochemistry 39*, 12632−12638.
23. Stellwagen, E., and Cass, R. (1974) *Biochem. Biophys. Res. Commun. 60*, 371−375.
24. Jordan, T., Eads, J. C., and Spiro, T. G. (1995) *Protein Sci. 4*, 716−728.
25. Indiani, C., De Sanctis, G., Neri, F., Santos, H., Smulevich, G., and Coletta, M. (2000) *Biochemistry 39*, 8234−8242.
26. Oellerich, S., Wackerbarth, H., and Hildebrandt, P. (2002) *J. Phys Chem B 106*, 6566−6580.
27. Dopner, S., Hildebrandt, P., Rosell, F. I., and Mauk, A. G. (1998) *J. Am. Chem. Soc. 120*, 11246−11255.
28. Zheng, J., Ye, S., Lu, T., Cotton, T. M., and Chumanov, G. (2000) *Bioploymers (Biospectroscopy) 57*, 77−84.
29. Shelnutt, J. A., Medforth, C. J., Berber, M. D., Barkigia, K. M., and Smith, K. M. (1991) *J. Am. Chem. Soc. 113*, 4077−4087.
30. Bushnell, G. W., Louie, G. V., and Brayer, G. D. (1990) *J. Mol. Biol. 214*, 585−595.
31. Hu, S., Morris, I. K., Singh, J. P., Smith, K. M., and Spiro, T. G. (1993) *J. Am. Chem. Soc. 115*, 12446−12458.
32. Smulevich, G., Bjerrum, M. J., Gray, H. B., and Spiro, T. G. (1994) *Inorg. Chem. 33*, 4629−4634.
33. Betz, S. F., and Pielak, G. J. (1992) *Biochemistry 31*, 12337−12344.
34. Pace, C. N. (1975) *CRC Crit. Rev. Biochem. 3*, 1−43.
35. Myers, J. K., Pace, C. N., and Scholtz, J. M. (1995) *Protein Sci. 4*, 2138−2148.
36. Sinibaldi, F., Fiorucci, L., Mei, G., Ferri, T., Desideri, A., Ascoli, F., and Santucci, R. (2001) *Eur. J. Biochem. 268*, 4537−4543.
37. Nicholson, R. S., and Shain, I. (1964) *Anal. Chem. 36*, 706−723.
38. Leszczynski, J. F., and Rose, G. D. (1986) *Science 234*, 849−855.
39. Sinibaldi, F., Howes, B. D., Smulevich, G., Ciaccio, C., Coletta, M., and Santucci, R. (2003) *J. Biol. Inorg. Chem.*, in press.
40. Assfalg, M., Bertini, I., Dolfi, A., Turano, P., Mauk, A. G., Rosell, F. I., and Gray, H. B. (2003) *J. Am. Chem. Soc. 125*, 2913−2922.
41. Banci, L., Bertini, I., Spyroulias, G. A., and Turano, P. (1998) *Eur. J. Inorg. Chem. 1*, 583−591.
42. Russell, B. S., Melenkivitz, R., and Bren, K. L. (2000) *Proc. Natl. Acad. Sci. U.S.A. 97*, 8312−8317.
43. Moore, G. R., and Pettigrew, G. W. (1990) *Cytochromes c. Evolutionary, Structural and Physicochemical Aspects*, Heidelberg, Germany, Springer-Verlag.
44. Berghuis, A. M., and Brayer, G. D. (1992) *J. Mol. Biol. 223*, 959−976.
45. Guex, N., and Peitsch, M. C. (1997) *Electrophoresis 18*, 2714−2723.

BI034132R